



POLITECNICO
MILANO 1863

RE.PUBLIC@POLIMI

Research Publications at Politecnico di Milano

Post-Print

This is the accepted version of:

M. Negrin, E. Macerata, G. Consolati, F. Quasso, A. Lucotti, M. Tommasini, L. Genovese, M. Soccio, N. Lotti, M. Mariani

Effect of Gamma Irradiation on Fully Aliphatic Poly(propylene/neopentyl Cyclohexanedicarboxylate) Random Copolymers

Journal of Polymers and the Environment, Vol. 26, N. 7, 2018, p. 3017-3033

doi:10.1007/s10924-018-1181-z

This is a post-peer-review, pre-copyedit version of an article published in Journal of Polymers and the Environment. The final authenticated version is available online at:

<https://doi.org/10.1007/s10924-018-1181-z>

Access to the published version may require subscription.

When citing this work, cite the original published paper.

Permanent link to this version

<http://hdl.handle.net/11311/1044069>



Effect of Gamma Irradiation on Fully Aliphatic Poly(Propylene/Neopentyl Cyclohexanedicarboxylate) Random Copolymers

M. Negrin¹ · E. Macerata¹ · G. Consolati² · F. Quasso² · A. Lucotti³ · M. Tommasini³ · L. Genovese⁴ · M. Soccio⁴ · N. Lotti⁴ · M. Mariani¹

© Springer Science+Business Media, LLC, part of Springer Nature 2018

Abstract

The widespread use of conventional petrochemical-based plastics and their low biodegradability led to a growing pollution issue. Among the class of the aliphatic polyesters, poly(propylene/neopentyl cyclohexanedicarboxylate) [P(PCE_xNCE_y)] random copolymers combine promising physical–chemical properties and biodegradability features but they are characterized by slow degradability. The effect of gamma radiation on both chemical-physical properties and compostability was evaluated by several techniques on different samples irradiated in air at absorbed doses up to 500 kGy and in water or under oxidative atmosphere up to 100 kGy. According to the results obtained, exposure to radiation significantly affects polymer molecular weight and hydrophilicity, while crystallinity remains unaltered and biodegradability is only slightly influenced. In particular, among the different irradiation environments used, irradiation in water seems to favor the polymer degradation in compost.

Keywords Aliphatic polyesters · Random copolymers · 1,4-Cyclohexanedicarboxylic acid · Gamma irradiation · Compostability

Introduction

Plastic pollution is one increasing issue due to the large amount of wastes that has been accumulating in the environment, caused by the long durability of conventional petrochemical-based plastics. In particular great concern has risen recently about the health and environmental effects caused by microplastics and their additives consumed by marine microorganisms that finally enter the food web [1–3]. Consequently, new synthetic materials more ecofriendly have

been studied [4], but the high production costs along with the poorer properties limit their introduction in the market. Aliphatic polyesters containing 1,4-cyclohexylene rings have attracted considerable attention as they combine the features of biodegradability with physical and chemical properties comparable with some of the most extensively used polymers, like LDPE, PP, etc. [5]. In addition, it was proved that the presence of an aliphatic ring along the polymer backbone confers high melting temperature, good thermal stability, good resistance to weather, heat, light and moisture, and interesting mechanical properties still maintaining biodegradability [6]. Different studies concern the effects of the introduction of 1,4-cyclohexylene rings into the polyester chains as a replacement of the aromatic moieties to increase the degradability [7–12, 9, 10, 11, 12]. Moreover, Commereuc et al. [12] showed that aliphatic cyclic units degrade after exposure to long UV degradation times.

Nowadays polymers could be exposed to radiation during their lifetime, e.g. for gamma sterilization. Ionizing radiation treatment of polymer materials can affect the polymer itself modifying its physical, chemical and biological properties due to its ability to cause crosslink or scission and oxidation of a wide range of materials [13]. It is well known that polymers containing aliphatic structure are sensible to

✉ M. Negrin
maddalena.negrin@polimi.it

¹ Department of Energy, Politecnico di Milano, Piazza L. da Vinci, 32, 20133 Milano, Italy

² Department of Aerospace Science and Technology, Politecnico di Milano, Piazza L. da Vinci, 32, 20133 Milano, Italy

³ Department of Chemistry, Material and Chemical Engineering “Giulio Natta”, Politecnico di Milano, Piazza L. da Vinci, 32, 20133 Milano, Italy

⁴ Department of Civil, Chemical, Environmental and Materials Engineering, Università di Bologna, Via Terracini, 28, 40131 Bologna, Italy

radiations [14, 15] but there are no systematic studies on the radiation induced effects in aliphatic polyesters containing cyclohexylene rings. The ionizing radiation effects on cyclic compounds lead to carbon-hydrogen bond breakage and, in the case of cyclohexane, the resulting molecular radicals disproportionate and the H atom mainly combines or undergoes H abstraction [16, 17].

The potential compostability is a key factor for the employment of new materials as packaging. The treatment with gamma radiation could facilitate the biodegradation of polymers by inducing its oxidative fragmentation [18–20]. The biodegradability of polyesters, due to the presence of hydrolysable ester bonds, depends on several factors but high molecular weights could extend the timescale of degradation. Although aliphatic polyesters are already characterized by the presence of many functional groups that assure the complete degradation under microbial attack, the kinetic of this process could be extremely slow, depending on many environmental factors such as temperature, humidity, pH and solar energy. The degradation process could be optimized and fastened but no attempts to exploit pre-irradiation for promoting biotreatment of these polyesters have been apparently made so far.

In this framework, the present research work focused on the evaluation of the effect of gamma radiation on chemical-physical properties of fully aliphatic poly(propylene/neopentyl glycol cyclohexanedicarboxylate) [P(PCE_xNCE_y)] random copolymers, reported in Fig. 1, whose general properties have been already presented in a previous paper [21]. The good processability of these polymers makes them good candidates for film applications, such as packaging, in which the materials can be treated with radiation before use and become waste in a short period. In this perspective, the experimental activities were addressed to investigate if a radiation treatment of the polymer in an environment promoting oxidative degradation could represent an effective pre-treatment for improving their biodegradation by inducing suitable structural modifications. For this purpose, samples were irradiated in air, oxygen atmosphere and water at absorbed doses up to several hundreds of kGy and then fully characterized by different analytical techniques.

Materials and Methods

Materials, Samples Preparation and γ -Irradiation

Poly(propylene cyclohexanedicarboxylate) and poly(neopentyl glycol cyclohexanedicarboxylate) homopolymers (PPCE and PNCE) and poly(propylene/neopentyl cyclohexanedicarboxylate) random copolymers [P(PCE_xNCE_y)] were synthesized according to the two-stage polymerization procedure previously reported by using *trans*-1,4-dimethylcyclohexane dicarboxylate (DMCE, 99%) [21]. Polymers, in form of powder, were molded into 1 mm thickness sheets and 200 μ m thickness films by first heating at 30 °C above the melting temperature and holding for 4 min and then increasing the molding pressure to 2 ton m⁻². The molds were immediately quenched at room temperature. Irradiation was carried out with a Co-60 gamma source with a dose rate of 2.5 kGy h⁻¹, allowing uniform exposure. Each sample was treated in air at adsorbed doses up to 500 kGy. A second irradiation campaign was performed plunging the samples into a fixed amount of deionized water or in oxygen atmosphere by applying absorbed doses up to 200 kGy. Finally, samples were characterized by gel permeation chromatography (GPC), differential scanning calorimetry (DSC), thermogravimetric analysis (TGA) and positron annihilation lifetime spectroscopy (PALS). The surface properties were investigated by water contact angle measurements (WCA) and scanning electron microscopy (SEM). Possible chemical changes were studied by infrared spectroscopy in attenuated total reflectance mode (FTIR-ATR). The degradation after irradiation was evaluated by disintegration tests based on the ISO-20200 standard method.

Molecular Weight

The weight average molecular weight (M_w) and number average molecular weight (M_n) were determined at 30 °C using a 1100 Hewlett Packard system equipped with a PL gel 5 m MiniMIX-C column (250 mm/4.6 mm length/i.d.). A refractive index detector was employed. In all cases, chloroform was used as eluent with a 0.3 mL min⁻¹ flow and

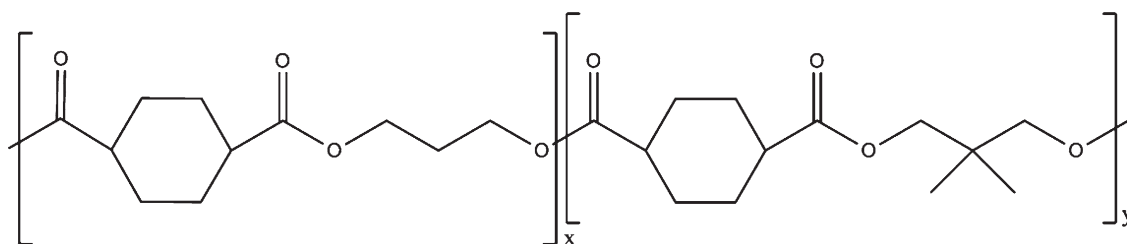


Fig. 1 Chemical structure of poly(propylene/neopentyl glycol cyclohexanedicarboxylate), P(PCE_xNCE_y)

130 sample concentrations of about 2 mg mL⁻¹ were applied.
 131 The calibration was done using polystyrene standards in
 132 the range of molecular weight 2000–100,000. Data were
 133 collected by HP Chemstation A.05.04 and elaborated with
 134 GPC Calculator 7.6 software. The measurements have been
 135 carried out in triplicate.

136 Thermal Properties

137 A Mettler Toledo differential scanning calorimeter (DSC
 138 822e) calibrated with high purity standards (indium and zinc)
 139 was used to evaluate thermal properties. Samples (c.a. 5 mg,
 140 200- μ m film or 1-mm sheet) were encapsulated in aluminum
 141 pans and heated to about 20 °C above melting temperature at
 142 a rate of 20 °C min⁻¹ (first scan) under nitrogen flux. For each
 143 sample, two heating and cooling cycles were performed. The
 144 glass transition temperature (T_g) was taken as the inflection
 145 point of the heat capacity increment Δc_p associated with
 146 the glass-to-rubber transition. The melting temperature
 147 (T_m) was determined as the peak value of the endothermic
 148 phenomenon. The melting enthalpy per unit mass (ΔH_m) was
 149 calculated from the area of the DSC endothermic peak. In
 150 addition, thermal stability of the polymers was studied using
 151 a Perkin Elmer TGA 4000 apparatus in nitrogen atmosphere
 152 (gas flow: 30 mL min⁻¹) at a heating rate of 10 °C min⁻¹ up
 153 to 850 °C. The temperature of initial decomposition (T_{id}) and
 154 of the maximum degradation rate (T_{max}) were determined.

155 Positron Annihilation Lifetime Spectroscopy

156 A conventional fast–fast coincidence time spectrometer with
 157 a time resolution of 250 ps was used for PALS measure-
 158 ments, in order to investigate the free volume features of
 159 the samples. The positron source (²²Na, activity 0.3 MBq)
 160 was deposited in an envelope of two Kapton® foils (7.5 μ m
 161 thick) and sandwiched between two samples of the investi-
 162 gated polymers. The samples thickness was enough to stop
 163 all the injected positrons. Three spectra of about 5×10^6
 164 counts were collected for each polyester at room tempera-
 165 ture. LT program [22] was used to analyze the spectra into
 166 three components allowing the determination of the lifetimes
 167 and the relative intensities.

168 Surface Characterization

169 In order to investigate the radio-induced modifications of
 170 polymers surface, chemical changes of polymer backbone,
 171 wettability and surface morphology were examined as a
 172 function of the absorbed dose.

173 FTIR analyses were carried out with a Nicolet Nexus
 174 FTIR spectrometer on pristine and irradiated samples of
 175 PPCE and P(PCE80NCE20). This apparatus was set up
 176 with a single bounce ATR probe made in silicon, which

177 allows the analysis of the surface of the polymer over the
 178 4000–700 cm⁻¹ wavenumber range. The ATR system is
 179 equipped with a load cell which allows to control the contact
 180 pressure of the ATR probe on the sample. Furthermore, a
 181 glass slide was placed between the load cell and the sample
 182 ensuring better contact between the film and the crystal, thus
 183 allowing the same depth to be analyzed for each sample. The
 184 penetration depth of IR light (1700 cm⁻¹) into the sample
 185 was estimated to be about 0.5 μ m. The infrared spectra were
 186 recorded after an accumulation of 32 scans with a resolution
 187 of 4 cm⁻¹. To make easier comparison, each spectrum was
 188 baseline corrected and the intensity of the whole spectrum
 189 was normalized to the reference peak at 1721 cm⁻¹,
 190 corresponding to the C=O stretching vibration.

191 Furthermore, in order to monitor changes in the wettability
 192 of polymers after irradiation, static water contact angle
 193 measurements were performed using an optical contact angle
 194 apparatus (OCA 15 Plus—Data Physics Instruments GmbH,
 195 Filderstadt, Germany) equipped with a video measuring
 196 system. Software SCA 20 (Data Physics Instruments GmbH,
 197 Filderstadt, Germany) was used for data acquisition. Prior
 198 to the analysis, the films surface was properly washed with
 199 70% ethanol aqueous solutions and then dried overnight in
 200 a sealed desiccator. Measurements were performed at ambient
 201 conditions by recording the side profiles of deionized water
 202 drops for image analysis. For each polymeric sample, ten
 203 measurements were performed. Image analysis was carried
 204 out with a Drop Shape Analysis software. The data reported
 205 correspond to the average values.

206 SEM images of polymers films were acquired using a
 207 field emission scanning electron microscope (FE-SEM)
 208 working in high vacuum Zeiss Supra 40 equipped with the
 209 GEMINI column. Images were acquired under vacuum by
 210 gluing films on aluminum stabs with carbon tape.

211 Disintegration Experiments Under Simulated 212 Composting Conditions

213 The disintegration experiments were performed on pristine
 214 and irradiated PPCE and P(PCE85NCE15) samples, following
 215 a procedure based on the ISO-20200 standard method. First,
 216 the initial mass of each sample was assessed placing it under
 217 vacuum to constant weight. Then, a weighted amount of
 218 mature compost was added to each specimen in a suitable
 219 vial and incubated at 58 °C for different periods, maintaining
 220 humidity at 90% of the water holding capacity of the system.
 221 The disintegration tests lasted from a minimum of 45 days up
 222 to 90 days. After the incubation period, samples were sieved
 223 at 2 mm, accurately washed by dipping in aqueous sodium
 224 dodecyl sulphate solution (2%) and finally dried under vacuum
 225 to constant mass. The disintegration in compost was evaluated
 226 on visual appearance and quantified by the determination
 227 of the samples weight loss. Further indications could be

228 deduced by SEM investigations. According to the standard
 229 method applied, the material can be defined disintegrable if
 230 the residual weight is under 30% after 45 days. To check the
 231 test effectiveness, multiple reference samples of Mater-Bi®,
 232 a compostable material produced by Novamont, were
 233 considered. All the tests have been performed in duplicate.

234 Results and Discussion

235 Physical Characterization

236 Sample irradiation was performed with a Co-60 gamma-ray
 237 source in air atmosphere on both films and sheets of PPCE
 238 and PPCE–P NCE copolymers. Some physical changes were
 239 observed in samples irradiated above 200 kGy, such as embrit-
 240 tlement. Figure 2 shows the residual number-average molecu-
 241 lar weight percentage values (M_n [%]) of PPCE and copolymers
 242 samples, together with the polydispersity index (PDI), as a
 243 function of the absorbed dose. The number-average molecular
 244 weight (M_n) of pristine samples ranges from about 25,000 to
 245 23,000 g mol^{-1} for PPCE and its copolymers with increasing
 246 the NCE co-unit percentage. In general, M_n strongly decreases
 247 with increasing the absorbed dose and PDI index increases.
 248 In the case of films, the residual number-average molecu-
 249 lar weight exhibits the same trend for all the samples, charac-
 250 terized by a change of slope just sketched beyond 150 kGy. As
 251 shown in Fig. 2 (top), at 200 kGy the M_n is almost halved and
 252 at 500 kGy the M_n [%] is around 20–30%. Lastly, no appreci-
 253 able copolymerization effect has been evidenced in the com-
 254 position range $0 < X_{\text{NCE}} < 0.2$.

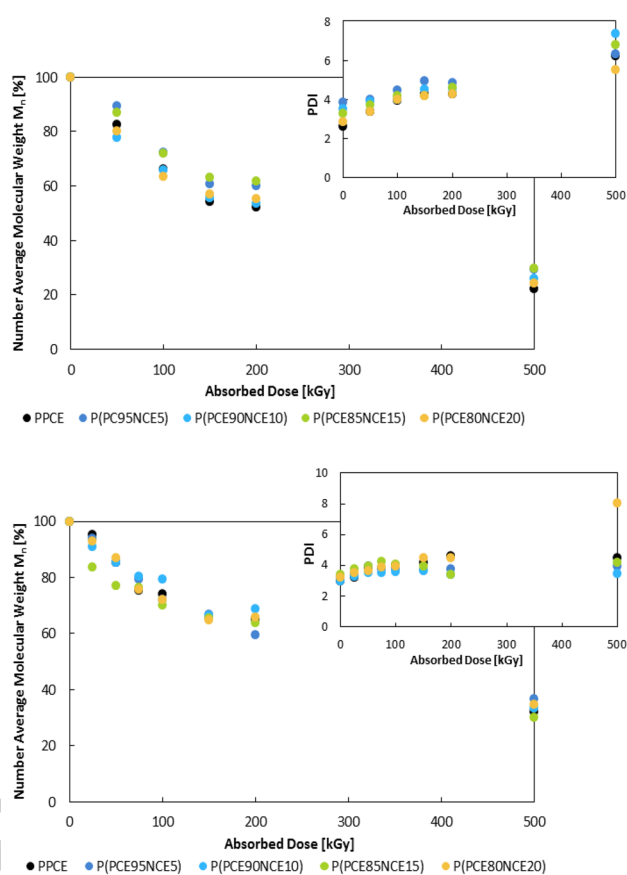
255 As expected, due to the different permeation of oxygen
 256 within the sample, a lower degradation is observed in the case
 257 of sheets with respect to films. The decrease of molecular
 258 weight is almost linear with the absorbed dose, displaying a
 259 even less noticeable change of slope over 150 kGy (see Fig. 2,
 260 bottom), linked to the increase of PDI. At 500 kGy the M_n [%]
 261 is around 30–40%.

262 The decrease of molecular weight is the result of two
 263 competing phenomena, cross-linking and chain scission,
 264 induced by exposure to high energy radiation. By using the
 265 molecular data, the yields of intermolecular crosslink G_x and
 266 scissioning G_s were calculated according to the following
 267 formulas [23–25]:

$$268 \frac{1}{M_w} = \frac{1}{M_{w,0}} + \frac{1}{2}(G_s - 4G_x)D_x \times 1.038 \times 10^{-7} \quad (1)$$

$$269 \frac{1}{M_n} = \frac{1}{M_{n,0}} + (G_s - G_x)D_x \times 1.038 \times 10^{-7} \quad (2)$$

270 where $M_{w,0}$ and $M_{n,0}$ are respectively the weight average and
 271 number average molecular weight of non-irradiated samples
 272 and M_w and M_n the corresponding values at the dose D_x
 273 expressed in kGy.



274 Fig. 2 GPC results: residual number-average molecular weight per-
 275 centage (M_n [%]) and polydispersity index (PDI) as a function of the
 276 absorbed dose and sample thickness: 200 μm (top) and 1 mm (bottom)

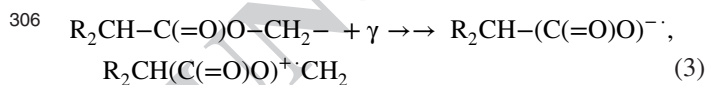
277 According to the values reported in Table 1, the G_s/G_x
 278 ratios are slightly higher than 4, without a clear trend
 279 with the absorbed dose, suggesting that chain scission is
 280 predominant and causes the M_n decrease despite crosslink
 281 is present. Chain branching arisen from cross-linking or
 282 radicals recombination leads to a less uniform distribution
 283 of chain length, as suggested by the increasing trend of PDI
 284 values for absorbed doses higher than 150 kGy (see Fig. 2).
 285 This kind of behavior was already observed and reported in
 286 literature for poly(alkylene dicarboxylate)s [26, 27]. Even
 287 if no further M_n reduction can be clearly observed with
 288 increasing NCE content, the presence of neopentyl glycol
 289 units could represent a weak point inside the copolymer
 290 structure, more prone to cleavage than propanediol subunit,
 291 and the recombination of radicals originated from the NCE
 292 unit could be limited by the presence of methyl groups
 293 and their steric hindrance. Moreover, the G_s/G_x ratios are
 slightly higher for films with respect to sheets, because of
 the lower oxygen permeation and thus the less oxidative
 conditions in the latter that favor crosslink.

Table 1 Yields of chain scission G_s and crosslinking G_x of polymer samples as a function of the absorbed dose and sample thickness

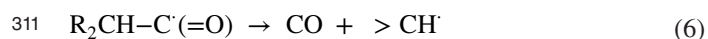
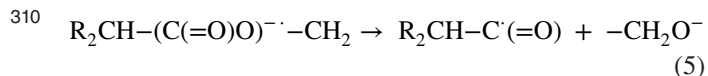
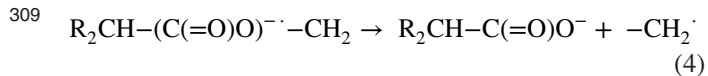
Polymer	Dose	1 mm			200 μ m		
		G_s	G_x	G_s/G_x	G_s	G_x	G_s/G_x
PPCE	50	1.78	0.39	4.57	3.93	0.79	4.94
	100	1.83	0.38	4.75	3.45	0.72	4.80
	150	1.86	0.42	4.41	3.38	0.69	4.90
	200	1.42	0.32	4.44	2.70	0.54	5.02
	500	2.29	0.54	4.25	3.68	0.76	4.87
P(PCE95NCE5)	50	1.80	0.40	4.50	1.34	0.25	5.43
	100	2.02	0.44	4.61	2.24	0.45	4.99
	200	1.83	0.43	4.29	1.93	0.39	4.95
	500	1.89	0.46	4.09	2.80	0.57	4.90
P(PCE90NCE10)	50	2.01	0.34	5.84	3.26	0.61	5.39
	100	1.54	0.29	5.30	2.95	0.52	5.71
	200	1.37	0.29	4.73	2.49	0.48	5.22
	500	2.47	0.57	4.33	3.40	0.74	4.60
P(PCE85NCE15)	50	3.23	0.84	3.85	1.78	0.42	4.21
	100	2.28	0.55	4.10	2.25	0.50	4.53
	200	1.51	0.38	3.98	1.80	0.40	4.49
	500	2.47	0.59	4.17	2.74	0.60	4.58
P(PCE80NCE20)	50	1.72	0.48	3.59	2.61	0.58	4.50
	100	2.07	0.46	4.50	3.01	0.67	4.50
	200	1.47	0.38	3.86	2.12	0.46	4.62
	500	2.06	0.49	4.20	3.19	0.63	5.03

294 Radiolytic Degradation Mechanism

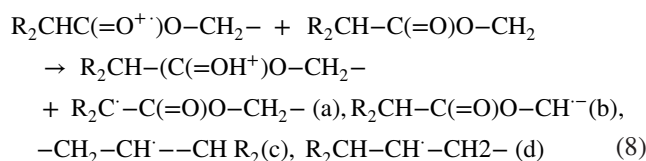
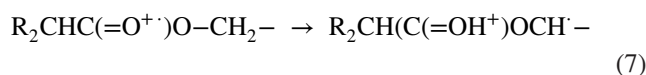
295 The radiolytic behavior of PPCE–PNCE copolymers can be
 296 inferred by studies conducted on the sub-units present in
 297 their structure. The radiolytic mechanism of simple carbox-
 298 ylic acids and esters proceeds via ionic and free radicals
 299 major pathways leading to a complex mixture of end prod-
 300 ucts which include carboxylic acids, alcohols, CO, CO₂, H₂
 301 and hydrocarbons [28–30]. The radiolytic behavior of the
 302 ester functional groups R₂CH–(C(=O)O)–CH₂– in the poly-
 303 mers and copolymers under study is suggested to proceed
 304 through electron capture and electron loss events, leading to
 305 the formation of anionic and cationic radicals:



307 The anionic radicals, R₂CH–(C(=O)O)^{·-}, proceed
 308 through chain scission according to the following reactions:

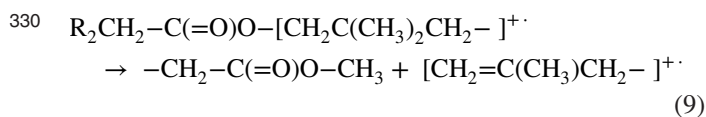


The cationic path instead envisages intramolecular
 and intermolecular H transfer according to the following
 reactions:

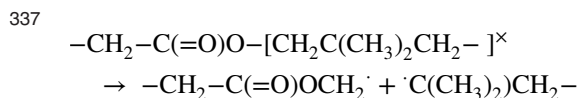
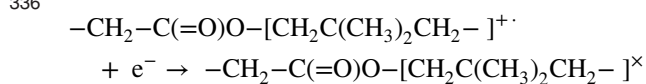


The H abstractions may not be restricted at the sites
 bearing the weakest C–H bonds (radicals a and b) but they
 may also take place at secondary C–H bonds within the
 propylene (radicals c) and cyclohexane (radicals d) sections
 being favored by the eventual juxtaposition of reacting
 centers in neighboring chains (intermolecular) or through
 the attainment of suited ring configurations (intramolecular).

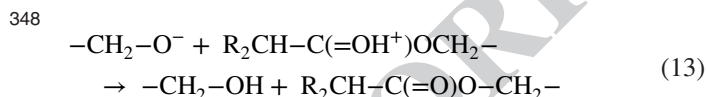
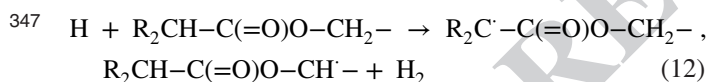
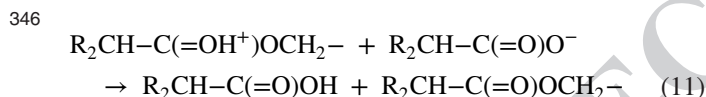
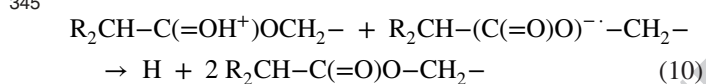
Despite GPC results did not clearly show that with
 increasing the NCE percentage chain scission increases
 over crosslinking, as compared to PPCE homopolymer, the
 neopentyl units in the PNCE homopolymer could display a
 higher cationic and excitation contributions to chain scission
 according to the following reaction:



331 The electron loss events localized in the neopentyl
332 moiety may have a role in prompting also the homolytic
333 chain scissions at the quaternary carbon following
334 charge neutralization and decomposition of the excited
335 intermediate:



338 In the solid polymer, bimolecular encounters via mass
339 diffusion are severely restricted, however charges migration
340 by electron hopping between neighboring centers may
341 occur even at the lowest temperature, as observed by EPR
342 measurements. A number of charge neutralization reactions
343 could be proposed leading to some of the expected major
344 stable end products:



349 The migration of free spins via a sequence of H
350 abstractions between reacting centers lying within a critical
351 distance is the basic mechanism allowing crosslinking and
352 branching to take place in the solid matrix during and after
353 the irradiation.

354 Radicals of type $R_2C \cdot -C(=O)O-CH_2-$ (a) are suited to
355 abstract hydrogen only from neighboring equivalent tertiary
356 C-H sites. As consequence, the spin migration is hindered,
357 the species have a longer lifetime and tend to accumulate
358 in the system, as clearly observed by means of matrix EPR
359 measurements in irradiated aliphatic polyesters. A similar
360 description applies, although to a lower extent, to the species
361 of type $-OCH \cdot -$ (b) for which spin migration is allowed
362 via thermoneutral (H abstraction at $-O-CH_2-$ sites) and
363 exothermic (H abstraction at $R_2CH-C(=O)O-$) reactions.
364 A different situation applies instead to the species

$-CH_2-CH-CHR_2$ (c) and $R_2CH-CH \cdot -CH_2-$ (d) which are
the most active in the spin migration process since they can
undergo exothermic or thermoneutral H abstractions with
all the C-H bonds in the polymer chains (except for methyl
C-H bonds). As a consequence, these species have a shorter
lifetime being terminated by coupling (crosslinks) or by
conversion to the other radical species. Two different stages
can thus be envisaged in the crosslinking process: (i) one
taking place during the irradiation and based on the coupling
of the "mobile" species (c) and (d) with themselves and with
the other species in the system; and (ii) a slower one taking
place mostly after the irradiation and during the degradation
of the polymer, and based mainly on the coupling of the
most stable species (a) and (b). The slower crosslinking
stage is likely to be less efficient since it is more exposed to
inhibition by oxygen. This scenario points to crosslinking
being favored by the greater relative abundance of mobile
radicals of type (c) and (d) which in turn implies a greater
concentration of methylene groups in the chains. This effect
may contribute, together with the better affinity for chain
scission, to enhance the G_s/G_x ratio in PNCE with respect
to PPCE.

Chain scission radicals $-CH_2 \cdot$ are the most reactive
species in the polymer system because of the favored
enthalpy changes in the H abstractions coupled with the
especially large motional amplitude available at the chain
ends. These species are of course expected to be the major
precursors of branching but they will also contribute to
the insource and post irradiation crosslinking processes
through the generation of intrachain radicals by H
abstraction.

Coupling takes place competitively with
disproportionation. The latter mechanism is generally
neglected despite the fact that the ratio between the
rate constants for the two reaction modes k_d/k_c attains
significant magnitudes which increase with increasing the
number of β hydrogens available for disproportionation and
it is relatively little affected by the change of solvents or
temperature [31]. In our polymers, a prominent contribution
by disproportionation can be predicted for reaction of
tertiary neopentyl radicals $-(CH_3)_2C \cdot -CH_2-$, since k_d/k_c
for t-butyl radical is reported to be 2.3. Disproportionation
is bound to reduce the crosslinking and branching yields,
but a partial compensation effect is expected to develop
with increasing the radiation dose following the generation
of double bonds. Disproportionation coupled with the
cage effect may be expected to enhance the yield of the
homolytic chain scissions by reducing the probability of the
back reaction. This effect is likely to acquire importance
when scissions of C-C bonds at the neopentyl units are
involved. As a consequence of the arrangement of the
neopentyl hydrocarbon structure to host the electron loss

417 centers, additional pathways for chain scission are available
 418 in PPCE–PNCE copolymers, based on the radical-cations
 419 fragmentation and excited intermediates. A lower yield
 420 of reactive radicals suited for carrying on crosslinking is
 421 produced due to the smaller number of CH₂ groups in the
 422 PNCE chains. With respect to PPCE, the greater affinity
 423 of neopentyl type radicals for disproportionation enhances
 424 the chain scission probability by hindering the cage back
 425 couplings.

426 Thermal Properties

427 It is known that the presence of the cyclohexylene
 428 ring along the polymer structure confers good thermal
 429 stability [10]. Moreover, as already reported, PPCE
 430 copolymerization with increasing percentage of NCE unit
 431 did not have a negative effect on the thermal properties.
 432 The effect of gamma irradiation on the thermal behavior
 433 was investigated on 1-mm sheets of PPCE homopolymer
 434 and the four copolymers.

435 The glass transition phenomenon is always slightly
 436 evident both in pristine and irradiated samples, due to
 437 relatively high degree of crystallinity. The glass transition
 438 temperature tends to become lower with irradiation dose in
 439 accordance with the molecular weight decrease and does not
 440 show a clear trend with NCE unit content (Table 2).

441 The melting process is characterized by two endothermic
 442 peaks, even in the unirradiated samples: the first one, with
 443 a lower melting enthalpy, lies between 50 and 60 °C; the
 444 second one is characterized by higher temperature and melt-
 445 ing enthalpy. This melting behavior is probably due to the
 446 existence of crystallites with different shape, dimension and
 447 degree of perfection [32]. In the crystalline phase, because of
 448 the additional restraint to molecular motion, chain scissions
 449 are hindered by the high probability of the back reactions,
 450 radicals and radical ions cannot easily attain their lowest
 451 energy configuration and bimolecular interactions between
 452 non-neighboring reactive centres are prevented. As a con-
 453 sequence, irradiation acts by creating defects which gener-
 454 ate less perfect crystallites. The first melting temperature
 455 increases with the absorbed dose due to reorganization of
 456 the chain segments. The second one decreases both with the
 457 dose, caused by chain scission that has taken place during
 458 irradiation creating shorter chains with increased ability to
 459 re-orientate, and with the NCE unit content as already found
 460 [21]. The thermograms of P(PCE90NCE10) as a function
 461 of the irradiation dose are reported as an example in Fig. 3.
 462 Finally, the melting enthalpy displays a decrease with the
 463 dose in the copolymers, with the exception of PPCE, and
 464 does not show a regular behavior with NCE unit content.
 465 Moreover, calorimetric measurements were performed on
 466 pristine and irradiated films of P(PCE95NCE5) and the
 467

Table 2 DSC thermal data (1st scan) for all the polymers sheets as a function of the absorbed dose

Dose (kGy)	0	75	200	500
PPCE				
T _g (°C)	15	11	12	10
T _m (°C)	52/150	56/144	59/142	60/136
ΔH (J/g)	34	35	38	37
P(PCE95NCE5)				
T _g (°C)	n.d	20	15	18
T _m (°C)	52/143	59/138	58/135	62/129
ΔH (J/g)	43	36	39	31
P(PCE90NCE10)				
T _g (°C)	19	16	17	13
T _m (°C)	53/136	55/132	57/129	60/123
ΔH (J/g)	38	36	36	34
P(PCE85NCE15)				
T _g (°C)	24	20	12	18
T _m (°C)	52/125	58/119	57/117	62/113
ΔH (J/g)	43	36	29	29
P(PCE80NCE20)				
T _g (°C)	17	15	15	12
T _m (°C)	62/120	55/114	57/113	60/109
ΔH (J/g)	32	31	31	30

n.d. not detectable

468 same changes on the melting temperatures and enthalpy were
 469 observed with respect to sheets.

470 The thermal stability of the samples under study was
 471 investigated by thermogravimetric analysis. From the
 472 TGA curves shown in Fig. 4, it can be noticed that in all
 473 cases the weight loss takes place in one step at decreasing
 474 temperatures with increasing the absorbed dose. T_{max}
 475 decreases of about 1.5 and 1% from the pristine sample to
 476 that irradiated at 500 kGy for PPCE and P(PCE80NCE20),
 477 respectively. The temperature of initial decomposition of
 478 pristine PPCE is 392 °C and decreases to 386 °C when
 479 irradiated at 500 kGy, and similarly T_{id} decreases from 395
 480 to 391 °C for the copolymer. Such results are in agreement
 481 with the molecular weight changes due to the degradation
 482 of polymer chains into shorter segments with lower
 483 decomposition temperatures.

484 Positron Annihilation Lifetime Spectroscopy

485 Exposure to physical factors such as ionizing radiation
 486 can lead to modifications of the free volume holes
 487 present in macromolecular matrices. In complementing
 488 conventional characterization techniques, PALS offers
 489 unique insights towards understanding molecular void
 490 spaces and microstructure, as well as changes in physical
 491 properties, such as gas and vapor permeability. The

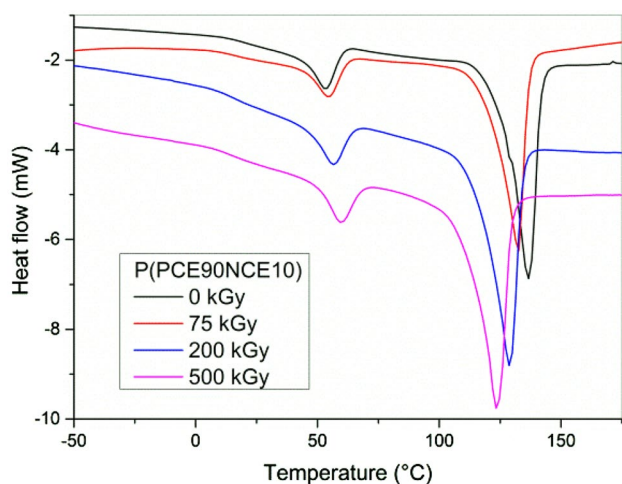


Fig. 3 DSC curves of P(PCE90NCE10) as a function of the irradiation doses

492 principles of positron annihilation in condensed matter
 493 have been extensively discussed elsewhere and here they
 494 are only briefly outlined [33, 34]. Positrons from a ^{22}Na
 495 source diffuse through the material and may bond with
 496 an electron, forming an exotic unstable atom named
 497 positronium (Ps), which gets trapped in a free volume
 498 hole. A typical annihilation time spectrum shows three
 499 components, corresponding to the main annihilation
 500 channels (para-Ps, free positrons and ortho-Ps). The
 501 longest component is due to the annihilation of ortho-
 502 positronium atom (o-Ps), the sublevel with parallel spins,
 503 into the holes present in the amorphous zones, therefore,
 504 it is used to probe the free-volume hole dimension. This
 505 involves a correlation between o-Ps lifetime and the sizes
 506 of the cavity, which can be cast in a quantitative form
 507 by suitably modeling the trapping site. A longer o-Ps
 508 lifetime τ_3 is found in bigger holes because the lower

electron density surrounding Ps reduces the probability
 of Ps annihilation. By assuming a spherical geometry a
 relationship between o-Ps lifetime τ_3 and the mean radius
 R of holes results, known as Tao-Eldrup equation [35,
 36]:

$$\tau_3 = \tau_0 \left[1 - \frac{R}{R + \delta R} + \frac{1}{2\pi} \sin \left(\frac{2\pi R}{R + \delta R} \right) \right]^{-1} \quad (14)$$

where $\delta R = 1.66 \text{ \AA}$ is an empirical parameter and τ_0
 (= 0.5 ns) is the annihilation lifetime of o-Ps in the presence
 of a high electron density. Cavities show a distribution of
 sizes, due to the disordered character of the amorphous
 zone. This involves a distribution of o-Ps lifetimes, which
 is supplied from the analysis of annihilation lifetime
 spectra. Holes size distribution is obtained through a simple
 mathematical treatment of the distribution of lifetimes [37].
 Table 3 reports centroid R and second moment σ of the
 normalized holes size distribution, as obtained from the
 PALS measurements. PPCE and copolymers display a small
 but significant decrease of the centroid of the distribution
 as the absorbed doses increase. On the other hand, no clear
 conclusion can be drawn as far as the second moment
 is concerned by taking into account the experimental
 uncertainties associated to the two parameters (2% for the
 centroid and 15% for the second moment). After exposure
 to ionizing radiation, the rearrangement of the broken
 chains is partially hindered by the steric hindrance of the
 methyl groups in the NCE co-unit affecting the sample
 crystallinity. Table 3 evidences a negative correlation
 between o-Ps intensity and the dose, which means a decrease
 in the formation probability of Ps. This could be related to
 the presence of carbonyl functional groups which increase
 with the dose. Positrons are attracted by these groups and
 annihilate with the corresponding electrons thus reducing
 o-Ps intensity.

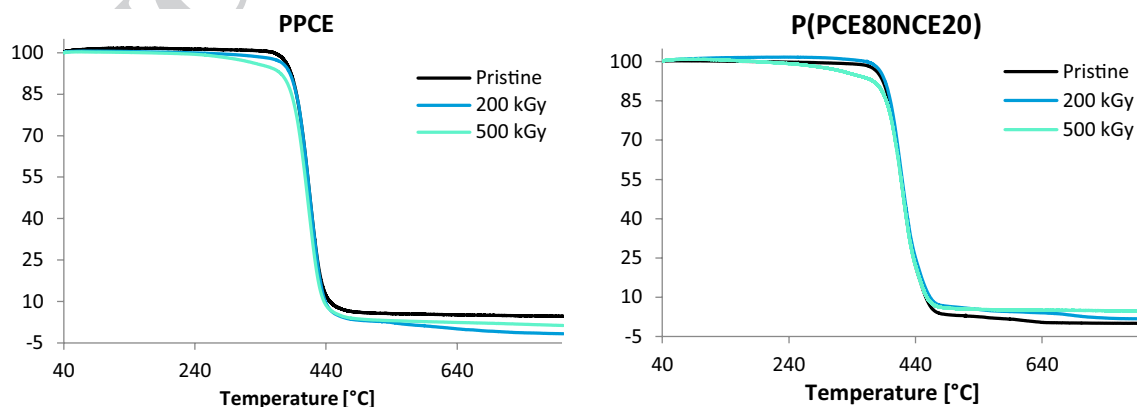


Fig. 4 Thermogravimetric curves of PPCE and P(PCE80NCE20) films at different absorbed doses

Table 3 PALS results on sheets: intensity of o-Ps decay (I_3), mean radius (R) of holes and relative dispersion (σ) as a function of the absorbed dose

Dose (kGy)	0	100	200	500
PPCE				
I_3 (%)	27.6	26.7	25.4	24.1
R (nm)	0.34	0.33	0.32	0.31
σ (nm)	0.06	0.06	0.05	0.05
P(PCE95NCE5)				
I_3 (%)	28.1	27.2	26.6	24.8
R (nm)	0.33	0.33	0.32	0.32
σ (nm)	0.06	0.06	0.05	0.05
P(PCE90NCE10)				
I_3 (%)	28.1	27.7	26.6	24.8
R (nm)	0.33	0.33	0.32	0.31
σ (nm)	0.06	0.06	0.06	0.05
P(PCE85NCE51)				
I_3 (%)	28.7	27.5	26.6	25.1
R (nm)	0.34	0.31	0.31	0.31
σ (nm)	0.06	0.05	0.05	0.05
P(PCE80NCE20)				
I_3 (%)	29.2	27.7	26.7	25.7
R (nm)	0.33	0.33	0.31	0.33
σ (nm)	0.06	0.06	0.05	0.06

Uncertainties of I_3 are evaluated to be around 5%

542 Surface Modifications

543 Since biodegradation in compost is a surface erosion
 544 process, it is important to understand in which way
 545 irradiation could affect the surface properties of a polymer,
 546 in particular those that could favor the microorganisms
 547 action, such as wettability. Oxidative degradation induced
 548 by radiation could lead to the formation of functional groups
 549 that can positively affect the polymer surface wettability.
 550 Therefore, possible chemical changes in treated films were
 551 qualitatively investigated by FTIR-ATR spectroscopy. To
 552 this purpose, the matrix containing the highest percentage
 553 of NCE sub-unit [P(PCE80NCE20)] was analyzed and
 554 compared with PPCE homopolymer. The FTIR spectra of
 555 PPCE did not show structural modifications after irradiation
 556 and, for sake of brevity, they are not reported here. Contrary
 557 to PPCE, for P(PCE80NCE20) some slight differences
 558 are visible in the fingerprint region and for the peak at
 559 1721 cm^{-1} , attributed to the carbonyl stretching vibration.
 560 We notice that the carbonyl stretching peak displays
 561 several overlapped components: with increasing dose, the
 562 component at the highest wavenumber (a) decreases, while
 563 the component at the lowest wavenumber (b) increases.
 564 This is more evident for the sample irradiated at 500 kGy
 565 (see Fig. 5). Such spectral changes have to be associated

to chemical modifications related with the formation of
 carbonyl groups placed in different positions than in the
 original polymer.

Relevant differences in the polymer wettability were
 evidenced by water contact angles (WCA) measurements
 on PPCE and copolymers films irradiated in air. As
 shown in Table 4, wettability is clearly enhanced only at
 500 kGy, coherently with what observed by FTIR analyses.
 WCA measurements were also acquired for PPCE and
 P(PCE80NCE20) films at low absorbed doses (25, 50 and
 100 kGy), highlighting an increase of even more than 10
 degrees with respect to the untreated samples (112 ± 2 for
 PPCE and 100 ± 2 for P(PCE80NCE20) at 25 kGy). It can
 be inferred that at such low absorbed doses radiation damage
 leads to a polymer surface with a hydrophobic character,
 while proceeding the irradiation such effect is balanced out
 by oxidation.

Radiation Effects on Compostability

Although aliphatic polyesters could potentially be
 biodegradable polymers, such characteristic strongly
 depends on their chemico-physical properties. PPCE and
 copolymers, despite the fully aliphatic structure and the
 presence of ester groups, are known to be slow degrading
 polymers [21]. The presence of the cyclohexylene ring
 in the polymers backbone confers to the materials under
 study all the peculiar features that make them suitable
 for technological applications, but at the same time
 provides good stability towards degradation in compost.
 In this perspective, it could be interesting to exploit the
 oxidative degradation induced by radiation to modify the
 polymer chemical structure and make it more prone to
 biodegradation, after the use so that not to affect the polymer
 performances.

Disintegration tests performed on irradiated PPCE and
 P(PCE85NCE15) films showed in general the low degree of
 disintegration of such matrices even at the highest absorbed
 doses, but also the promising improvement in degradation
 of the irradiated samples with respect to the pristine ones.
 As reported in literature, weight losses of about 3% for
 pristine PPCE and 8% for pristine P(PCE85NCE15) were
 obtained after 140 days of incubation [21]. In the present
 work, it was demonstrated that after 45 days of incubation
 all the pristine samples were barely attacked by microor-
 ganisms showing a weight loss under 1%, while samples
 irradiated at 500 kGy reached a weight loss of about 5% for
 PPCE and 12% for P(PCE85NCE15). In order to develop
 a radiation treatment as eco-friendly and cost-effective
 as possible, attempts were made to try to reach the same
 degree of disintegration with a lower absorbed dose. In this
 perspective, disintegration tests were repeated on samples
 irradiated up to 200 kGy and the test duration was extended

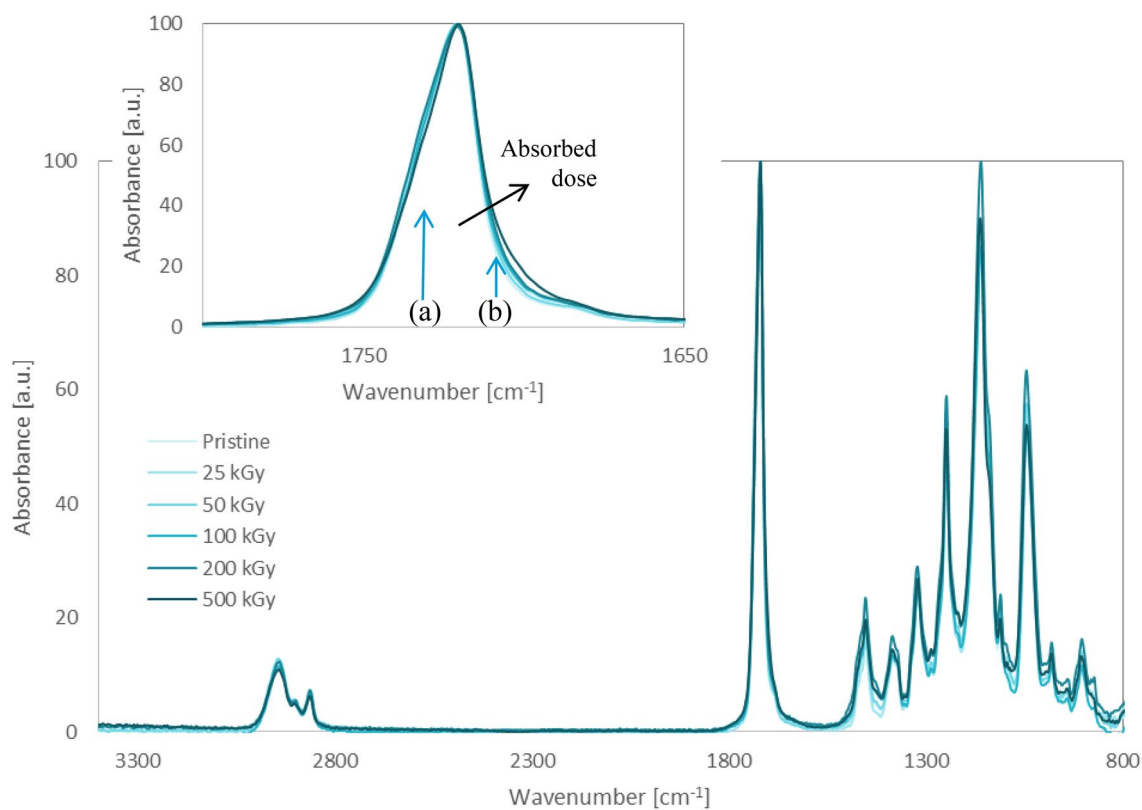


Fig. 5 ATR-FTIR spectra of P(PCE80NCE20) films, pristine and irradiated at absorbed doses up to 500 kGy. The spectra have been normalized such that the intensity of the strongest peak is 100

Table 4 Water contact angles for PPCE and copolymers 200 μm films as a function of the absorbed dose

Polymer	Contact angle ($^{\circ}$)		
	Pristine	200 kGy	500 kGy
PPCE	94 ± 3	98 ± 2	87 ± 1
P(PCE95NCE5)	98 ± 2	98 ± 2	88 ± 2
P(PCE90NCE10)	96 ± 2	96 ± 1	87 ± 3
P(PCE85NCE15)	92 ± 1	89 ± 1	85 ± 1
P(PCE80NCE20)	88 ± 2	87 ± 2	74 ± 1

617 to 70 and 90 days. As reported in Fig. 6, in comparison
 618 with the tests at 45 days, after 70 days the degradation
 619 of pristine samples does not show improvements, while
 620 PPCE and P(PCE85NCE15) irradiated in air at 200 kGy
 621 exhibit a weight loss of about 4 and 16%, respectively. The
 622 experiments performed demonstrated that the same result
 623 in terms of weight loss was obtained by more than halving
 624 the absorbed dose and less than doubling the incubation
 625 time. After 90 days in compost no relevant improvements
 626 can be reached with respect to 70 days tests.

627 Morphological modifications of irradiated polymers after
 composting were investigated by SEM. As an example, SEM

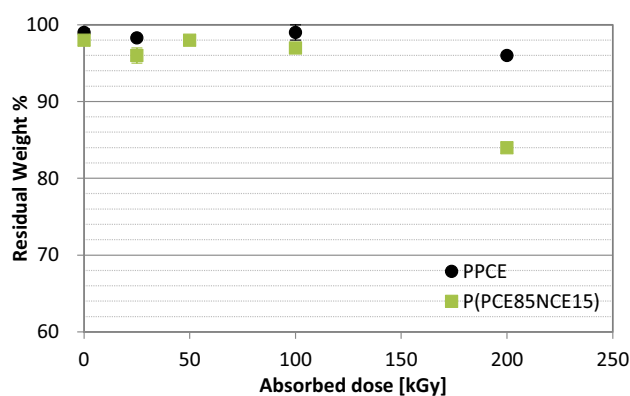


Fig. 6 Residual weight % as a function of the absorbed dose for 200 μm films of PPCE and P(PCE85NCE15) copolymer irradiated in air after 70 days in compost

628 micrographs of PPCE and P(PCE85NCE15) films after
 629 70 days of composting are reported in Fig. 7. Micrographs
 630 show superficial modifications already at low absorbed doses
 631 (25 kGy), mainly as for the copolymer surface is concerned.
 632 At higher absorbed doses cracks and holes appear on the
 633 surface, whose intensity increases with the irradiation dose,

634 leading to a remarkable damage of the surface, especially
635 for the copolymer, that clearly evidence the proceeding of
636 the degradation process. The formation of cracks and holes
637 is faster and more evident for the copolymer with respect
638 to the homopolymer, in accordance with the weight loss
639 measurements.

641 Effect of Irradiation Environment

642 In order to maximize the radiation effects on materials, two
643 additional irradiation environments were considered, i.e.
644 water and oxygen atmosphere. As reported in literature,
645 irradiation of polymers in dilute water solutions greatly
646 increases the crosslinking yield because of the obliteration
647 of the direct radiolysis effects and its substitution with the
648 reactions of species (OH^\cdot and H^\cdot radicals) with great affinity
649 for H abstraction [25]. Previous radiolysis studies on model
650 systems or similar systems, such as low molecular weight
651 alkanes in water [38–41] and hydrophilic polymers in water
652 [42–44] have shown that the HO^\cdot radical is the main species
653 responsible for the degradation of these materials. In the
654 present case, direct radiolysis effects on the polymers are
655 still important and the mechanism described by Charlesby
656 can be envisaged being significant only at the surface [25].
657 During irradiation, the presence of water at the surface of
658 the polymer involves specific radical reactions among the
659 species coming from water radiolysis (OH^\cdot and H^\cdot radicals)
660 and polymers radicals. It is clear that such reactions could
661 lead to relevant surface modifications that can strongly affect
662 the hydrophilicity of the polymer surface and thus favor its
663 attack by microorganisms. Therefore, some attempts were
664 performed to find the conditions under which such effect is
665 maximized keeping the absorbed dose as low as possible.
666 Moreover, since it is well known that oxygen radicals are
667 very reactive species, irradiation in oxygen atmosphere
668 was attempted in order to try to exploit the most extreme
669 oxidative conditions to modify polymer structure and surface
670 properties.

670 Given the large number of samples required by such
671 kind of experimental study, investigations on the effect of
672 radiation environment were preliminary conducted only on
673 the homopolymer and two copolymers and at few selected
674 absorbed doses. In particular, the two copolymers with the
675 highest NCE percentage were considered. Figure 8 reports
676 the GPC results for PPCE and P(PCE80NCE20) films irra-
677 diated in water and oxygen atmosphere up to 200 kGy and
678 the molecular data for P(PCE85NCE15) films irradiated
679 in water up to 100 kGy. No significant differences were
680 observed in comparison with films irradiated in air. In some
681 cases, irradiation in air seems to be the most effective one
682 in terms of molecular weight reduction. In particular, the
683 oxygen atmosphere at high absorbed doses leads to a lower
684 decrease of M_n [%] with a more homogeneous distribution

of chain length (lower PDI values) with respect to irradiation
in air.

For PPCE films irradiation at 100 kGy in water led
to changes in the thermal properties comparable to
those observed after irradiation in air. In the case of the
copolymer P(PCE85NCE15), T_m and ΔH_m vary differently
when irradiated in water with respect to irradiation in air:
at 100 kGy T_m varies from 123 °C in the pristine sample
to 122 and 118 °C when irradiated in air and water,
respectively, while the melting enthalpy increases from
23 J g⁻¹ to 29 and 25 J g⁻¹. The presence of the NCE
sub-unit in the copolymer resulted in a higher sensibility
to the irradiation environment. The calorimetric curves
obtained for PPCE and P(PCE80NCE20) films irradiated
in air, water and oxygen at 25 kGy highlighted that, despite
the low absorbed dose, crystallinity was enhanced in all
the cases.

Up to 100 kGy FTIR-ATR investigations and
WCA measurements on PPCE, P(PCE85NCE15) and
P(PCE80NCE20) films did not highlight differences
between the irradiation environments. As shown in
Table 5, it is worth noting that in the case of irradiation
in water the increase of the polymers hydrophobic character
observed after irradiation in air in the absorbed dose range
25–100 kGy was no more evident, while it is still present
in the sample irradiated in oxygen at 25 kGy. (112 ± 2 for
PPCE and 100 ± 2 for P(PCE80NCE20) at 25 kGy).

As shown in Fig. 9, the results obtained in the
disintegration experiments indicated that irradiation in
water at the considered absorbed doses was not significantly
effective in enhancing the rate of degradation of the polymers
under study. Indeed, after 70 days in compost PPCE and
P(PCE85NCE15) samples irradiated in water showed a
maximum weight loss of about 4% at 100 kGy, similar to
that reached by irradiation in air. The corresponding SEM
images show how the degradation process by microorganisms
is acting on the polymer surface leading to the appearance
of irregular zones. In particular, PPCE surface seems to be
consumed more uniformly with hollowed zones, as clearly
shown in Fig. 10.

Concerning PPCE degradation irradiation in oxygen
as well as the extension of test duration did not imply
significant improvements (see Table 6), with respect to
the results already presented. Although P(PCE80NCE20)
films irradiated at 25 kGy in oxygen showed the same
molecular weight decrease observed after irradiation in
air and water, no substantial variations of the thermal
properties and a worsen wettability, preliminary
disintegration tests highlighted a progressive decrease of
few percent of the residual weight after 70 and 90 days.
As shown in Table 6, P(PCE80NCE20) sample irradiated
in water shows the lowest residual weight after 70 days.
Disintegration experiments prolonged to 90 days seems to

Fig. 7 SEM micrographs of PPCE and P(PCE85NCE15) samples irradiated at 25, 100 and 200 kGy in air and kept for 70 days in compost (magnification $\times 5000$)

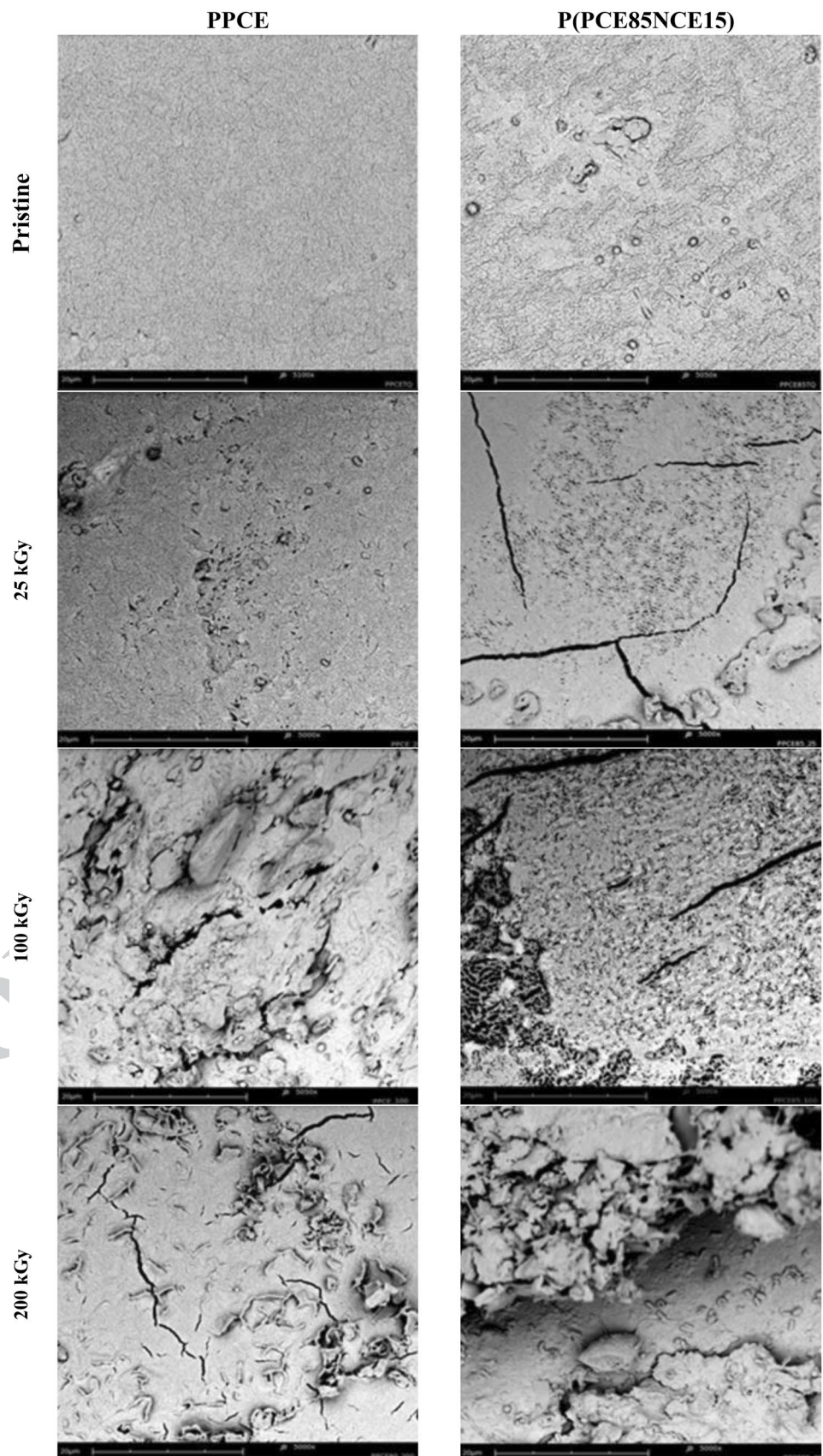
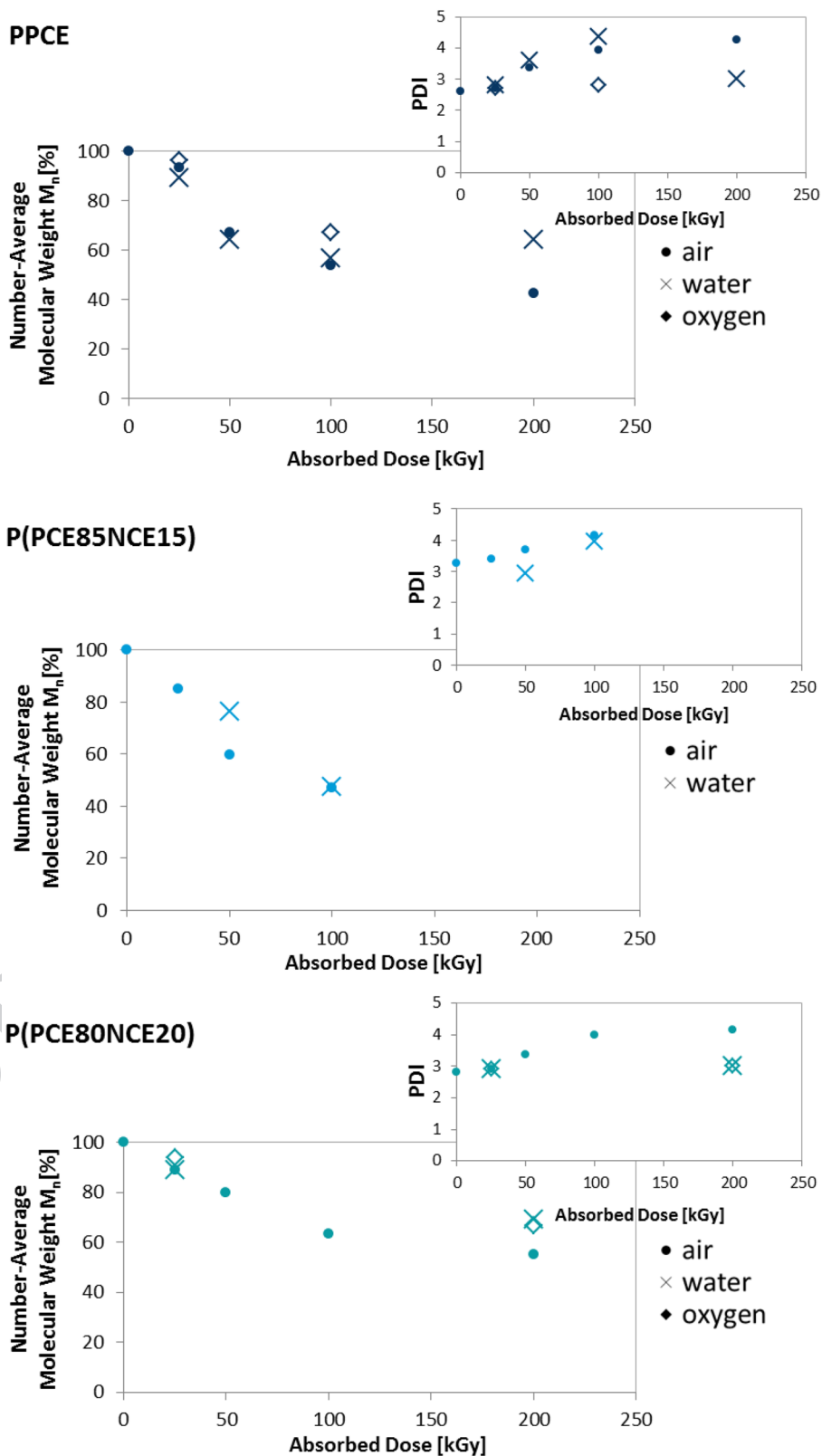


Fig. 8 GPC results on 200 μm films: residual number-average molecular weight M_n [%] and polydispersity index (PDI) as a function of the absorbed dose and irradiation environment



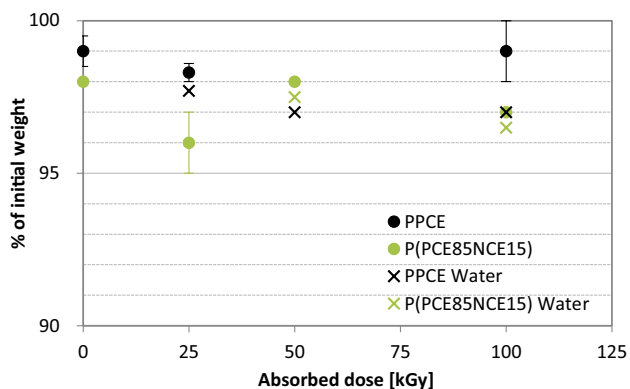
738 suggest a different disintegration rate among the differ-
 739 ent irradiation environments. Indeed, while the residual
 740

weight of the sample irradiated in water remains constant,
 that of P(PCE80NCE20) sample irradiated in oxygen
 decreases.

741
 742
 743

Table 5 Water contact angle versus absorbed dose for PPCE and copolymers 200 μm films irradiated in water

Polymer	Contact angle ($^\circ$)			
	Pristine	25 kGy	50 kGy	100 kGy
PPCE	94 ± 3	101 ± 3	94 ± 1	98 ± 2
P(PCE85NCE15)	92 ± 1	–	98 ± 4	97 ± 7
P(PCE80NCE20)	88 ± 2	89 ± 2	–	85 ± 4

**Fig. 9** Residual Weight % as a function of the absorbed dose for 200 μm films of PPCE and P(PCE85NCE15) copolymer irradiated in air and water after 70 days in compost

744 Despite the small weight losses, some evidences of degradation can be observed for PPCE in the samples irradiated in oxygen and especially in water (see Fig. 11).
 745
 746 Interestingly, in P(PCE80NCE20) copolymer small holes appear when the sample is irradiated in air and oxygen, becoming larger if the sample is irradiated in water. The
 747
 748
 749

750 peculiar morphological modifications observed for the samples irradiated in water with respect to the other irradiation environments are coherent with the wettability changes obtained by WCA measurements. This could be an indication that a degradation process, even if slow, has already started in the irradiated samples after 70 days of composting, while the pristine samples surfaces remain practically unchanged. Figure 12 clearly demonstrate the evolution of the degradation process on P(PCE80NCE20) films increasing the incubation period up to 90 days: the sample irradiated in water shows smaller holes uniformly distributed on the surface, while the one treated in oxygen atmosphere exhibits bigger holes inside hollowed areas.

751
 752
 753
 754
 755
 756
 757
 758
 759
 760
 761
 762
 763
 764
 765
 766
 767

Conclusions

768
 769
 770
 771
 772
 773
 774
 775
 776
 777
 778
 779

The present work investigated the behavior under gamma irradiation of new PPCE-based random copolymers, containing cyclohexane unit, whose general properties make them good candidates for biodegradable packaging applications. Indeed, they show good thermal and barrier properties and a slow biodegradation rate. In this perspective, the research activity focused on how gamma radiation can affect the polymer degradability in compost.

Experimental investigations highlighted that exposure to gamma radiation in air mainly affects the polymer

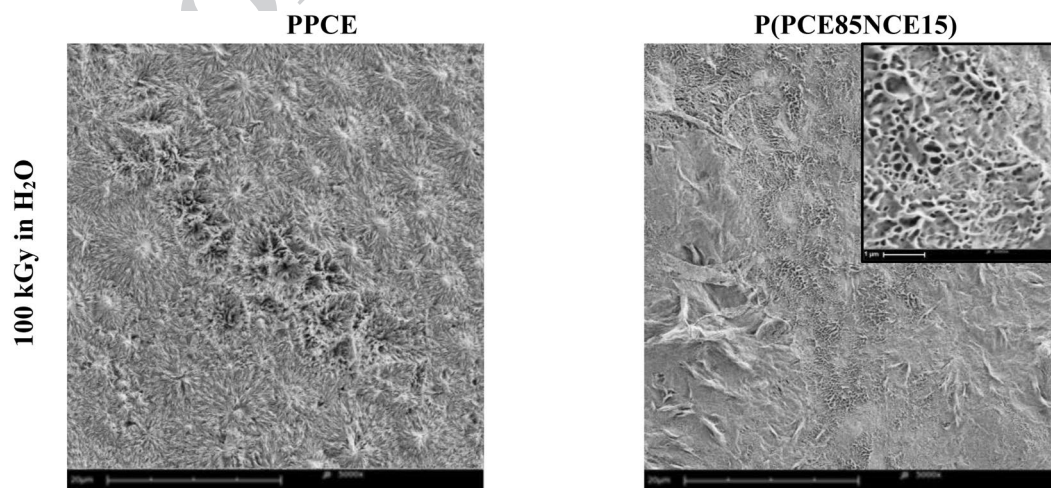
**Fig. 10** SEM micrographs of PPCE and P(PCE85NCE15) irradiated at 100 kGy in water and analyzed after 70 days of composting (magnification $\times 5000$, insert $\times 50000$)

Table 6 Results of disintegration tests (70 and 90 days) on PPCE and P(PCE80NCE20) films irradiated at 25 kGy in the different irradiation environments

Residual weight %				
Incubation period, day	Pristine	Irradiated at 25 kGy in		
		Air	Water	Oxygen
PPCE				
70	99 ± 0.5	98.5 ± 0.5	97.5 ± 0.5	97 ± 0.5
90	99 ± 0.1	97.5 ± 0.5	97.5 ± 0.5	97 ± 0.1
P(PCE80NCE20)				
70	97 ± 1	98.5 ± 0.5	94.5 ± 0.5	97.5 ± 0.5
90	97 ± 1	96.1 ± 0.5	94.5 ± 1	94 ± 2

780 molecular weight. The radicals formed during irradiation
 781 follow mainly a chain scission mechanism causing
 782 a decrease of the molecular weight in all the dose range
 783 considered. Nevertheless, the treated samples maintained
 784 a good thermal stability and exhibited an increased hydro-
 785 philicity for absorbed doses above 200 kGy. These find-
 786 ings suggest that the irradiated samples should be more
 787 prone to biodegradation. Indeed, despite the relatively

788 short period of incubation considered, SEM images clearly
 789 show significant surface changes in the treated samples
 790 and irradiation in air at 200 kGy succeeded in enhanc-
 791 ing the rate of degradation for P(PCE85NCE15) films:
 792 the pristine samples showed a weight loss within 1% after
 793 70 days, while the P(PCE85NCE15) films irradiated at
 794 200 kGy showed a weight loss around 16% over the same
 795 incubation time.

796 In order to enhance the radiation damage, two attempts
 797 were performed by considering (i) a more reactive oxygen
 798 atmosphere, which favors degradation by oxidation, and (ii)
 799 irradiation in solution, which should strongly affect polymer
 800 surface. The experimental activities showed that such irradi-
 801 ation environments led to positive effects on the degradation
 802 in compost. Indeed, a weight loss of about 6% was obtained
 803 on P(PCE80NCE20) films irradiated at 25 kGy in water and
 804 oxygen after 70 and 90 days of composting, respectively.

805 Further experimental investigations are already in pro-
 806 gress to demonstrate the effectiveness of irradiation under
 807 more oxidative conditions to improve polymers degrada-
 808 tion rate in compost.
 809

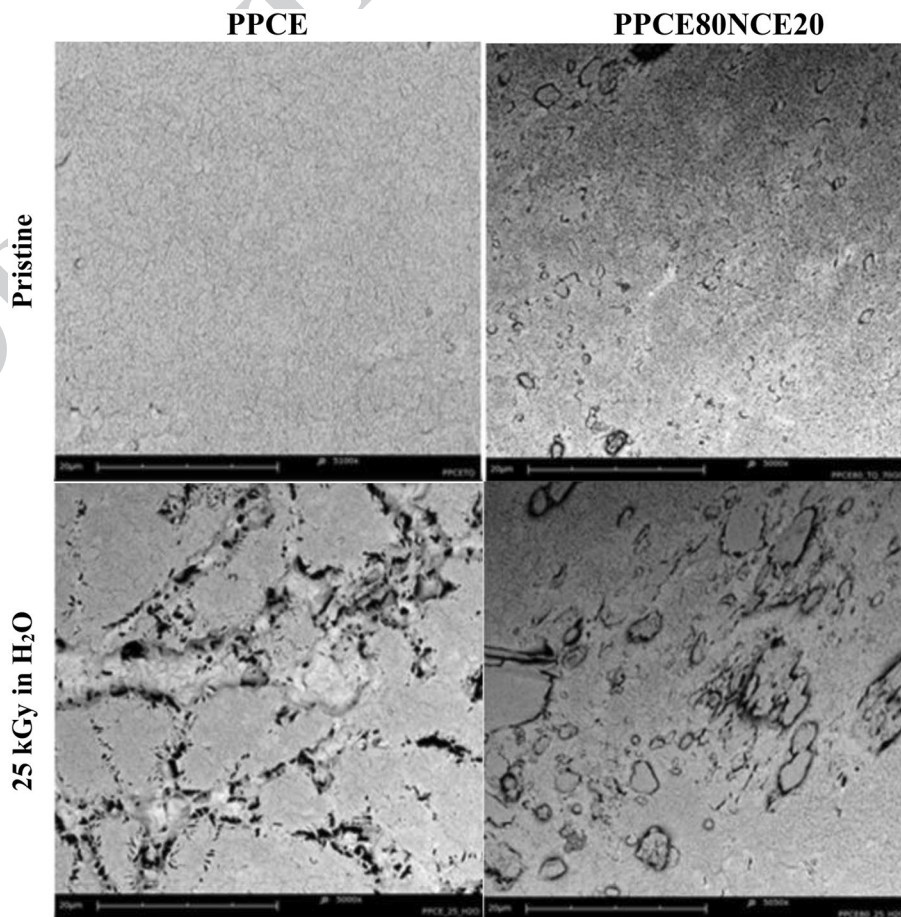
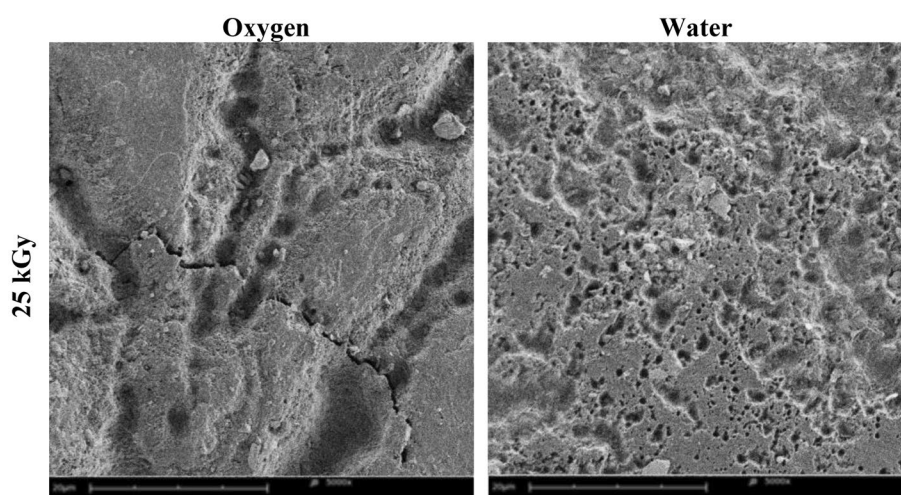
Fig. 11 SEM micrographs of PPCE and P(PCE80NCE20) irradiated at 25 kGy in water after 70 days of composting (magnification ×5000)

Fig. 12 SEM micrographs of P(CE80NCE20) irradiated at 25 kGy in different environment and analyzed after 90 days of composting (magnification $\times 5000$)



810 **Acknowledgements** Authors would like to thank Prof. Antonio Fau-
811 caitano for the fruitful discussion on the radiolytic degradation mecha-
812 nisms of the system under study. The authors are grateful to Gam-
813 matom S.r.l. for the precious support in the irradiation experiments.
814

References

- 815
- 816 1. Mackay K, Afonso A, Maggiore A, Binaglia M (2016) Extensive
817 review on the presence of microplastics and nanoplastics in sea-
818 food: data gaps and recommendations for future risk assessment
819 for human health. Fate and impact of microplastics in marine eco-
820 systems MICRO2017
 - 821 2. Thompson RC (2015) Microplastics in the marine environment:
822 sources, consequences and solutions. In: Bergmann M, Gutow L,
823 Klages M (eds) Marine anthropogenic litter
 - 824 3. Wright SL, Thompson RC, Galloway TS (2013) The physical
825 impacts of microplastics on marine organisms: a review. *Environ*
826 *Pollut* 178:483–492
 - 827 4. Vert M (2005) Aliphatic polyesters: great degradable polymers
828 that cannot do everything. *Biomacromolecules* 6:538–546
 - 829 5. Tokiwa Y, Calabia BP, Ugwu CU, Aiba S (2009) Biodegradability
830 of plastics. *Int J Mol Sci* 10:3722–3742
 - 831 6. Collyer AA (1990) A Practical guide to the selection of high-
832 temperature engineering thermoplastics. Elsevier, Burlington,
833 p 66
 - 834 7. Sánchez-Arrieta N, Martínez de Ilarduya A, Alla A, Muñoz-
835 Guerra S (2005) Poly(ethylene terephthalate) polymers containing
836 1,4-cyclohexane dicarboxylate units. *Eur Polym J* 41:1493–1501
 - 837 8. Wang L, Xie Z, Bi X, Wang X, Zhang A, Chen Z, Zhou J, Feng
838 Z (2006) Preparation and characterization of aliphatic/aromatic
839 copolyesters based on 1,4-cyclohexanedicarboxylic acid. *Polym*
840 *Degrad Stab* 91(9):2220–2228
 - 841 9. Sandhya TE, Ramesh C, Sivaram S (2007) Copolyesters based on
842 poly(butylene terephthalate)s containing cyclohexyl and cyclopentyl
843 ring: effect of molecular structure on thermal and crystallization
844 behavior. *Macromolecules* 19(40):6906–6915
 - 845 10. Berti C, Binassi E, Celli A, Colonna M, Fiorini M, Marchese
846 P, Marianucci E, Gazzano M, Di Credico F, Brunelle DJ (2008)
847 Poly(1,4-cyclohexylenedimethylene 1,4-cyclohexanedicarboxy-
848 late): influence of stereochemistry of 1,4-cyclohexylene units
849 on the thermal properties. *J Polym Sci B* 46:619–630
 - 850 11. Berti C, Celli A, Marchese P, Barbiroli G, Di Credico F,
851 Verne V, Commereuc S (2009) Novel copolyesters based on
852 poly(alkylene dicarboxylate)s: 2. Thermal behavior and bio-
853 degradation of fully aliphatic random copolymers containing
854 1,4-cyclohexylene rings. *Eur Polym J* 45:2402–2412
 - 855 12. Commereuc S, Askanian H, Verney V, Celli A, Marchese P,
856 Berti C (2013) About the end life of novel aliphatic and ali-
857 phatic-aromatic (co)polyesters after UV-weathering: structure/
858 degradability relationships. *Polym Degrad Stab* 98:1321–1328
 - 859 13. Burillo G, Clough R, Czvikovszky T (2002) Polymer recycling:
860 potential application of radiation technology. *Radiat Phys Chem*
861 64:41–51
 - 862 14. Buttafava A, Consolati G, Mariani M, Quasso F, Ravasio U
863 (2005) Effects induced by gamma irradiation of different poly-
864 esters studied by viscosimetry, thermal analysis and positron
865 annihilation spectroscopy. *Polym Degrad Stab* 89:133–139
 - 866 15. Ravasio U, Buttafava A, Mariani M, Dondi D, Faucitano A
867 (2008) EPR and ab-initio study on the solid state radiolysis of
868 aliphatic and aromatic polyesters. *Polym Degrad Stab* 93:1031
 - 869 16. Stone JA (1967) Radiolysis of cyclohexane in a xenon matrix at
870 77 K. *Can J Chem* 46(8):1267–1277
 - 871 17. LaVerne JA, Enomoto K, Araos MS (2007) Radical yields
872 in the radiolysis of cyclic compounds. *Radiat Phys Chem*
873 76(8–9):1272–1274
 - 874 18. Shah AA, Hasan F, Hameed A, Ahmed S (2008) Biological
875 degradation of plastics: a comprehensive review. *Biotechnol*
876 *Adv* 26:246–265
 - 877 19. Arkatkar A, Arutchelvi J, Sudhakar M, Bhaduri S, Uppara PV,
878 Doble M (2009) Approaches to enhance the biodegradation of
879 polyolefins. *Open Environ Eng J* 2:68–80
 - 880 20. Negrin M, Macerata E, Consolati G, Quasso F, Genovese L,
881 Soccio M, Giola M, Lotti N, Munari A, Mariani M (2017)
882 Gamma radiation effects on random copolymers based on
883 poly(butylene succinate) for packaging applications. *Radiat*
884 *Phys Chem (in press)*
 - 885 21. Genovese L, Lotti N, Gazzano M, Finelli L, Munari A (2015)
886 New eco-friendly random copolyesters based on poly(propylene
887 cyclohexanedicarboxylate): structure-properties relationships.
888 *Express Polym Lett* 9:972–983
 - 889 22. Kansy J (1996) Microcomputer program for analysis of positron
890 annihilation lifetime spectra. *Nucl Instrum Methods Phys*
891 *Res A* 374:235–244
 - 892 23. O'Donnell JH (1991) Chemistry of radiation degradation of pol-
893 ymers. In: Clough R (ed) Radiation effects on polymers. ACS

- 892 symposium series, American Chemical Society, Washington, DC, 925
893 pp 402–413 926
894 24. Olejniczak J, Rosiak J, Charlesby A (1991) Gel/dose curves for 927
895 polymers undergoing simultaneous cross-linking and scission. 928
896 Radiat Phys Chem 38(1):113–118 929
897 25. Charlesby A (1960) Atomic radiation and polymers. Pergamon 930
898 Press, Oxford 931
899 26. Gupta MC, Deshmukh VG (1982) Radiation effects on poly(lactic 932
900 acid). Polymer 24:827–830 933
901 27. Loo JSC, Ooi CP, Boey FYC (2005) Degradation of poly(lactide- 934
902 co-glycolide) (PLGA) and poly(l-lactide) (PLLA) by electron 935
903 beam radiation. Biomaterials 26:1359–1367 936
904 28. Mičić OI, Gal OS (1979) Radiation chemistry of acids, esters, 937
905 anhydrides, lactones and lactams, In: Patai S (ed) Acid deriva- 938
906 tives, vol 2. Wiley, Chichester 939
907 29. Sevilla MD, Becker D, Sevilla CL, Plante K, Swarts S (1984) An 940
908 electron spin resonance investigation of ester cation radicals at 941
909 low temperatures. Faraday Discuss Cem Soc 78:71–81 942
910 30. Emanuel NM, Roginskii VA, Buchachenko AL (1982) Some prob- 943
911 lems of the kinetics of radical reactions in solid polymers. Russ 944
912 Chem Rev 51(3):203 945
913 31. Ingold KU (1973) Rate constants for free radical reactions. In: 946
914 Kochi JK (ed) Free radicals, vol 1. Wiley, New York 947
915 32. Kenney JF (1968) Properties of block versus random copolymers. 948
916 Polym Eng Sci 8:216–226 949
917 33. Wang SJ, Jean YC (1988) Positrons and positronium in molecular 950
918 solids. In: Schrader DM, Jean YC (eds) Positron and positronium 951
919 chemistry. Elsevier, Amsterdam, The Netherlands, pp 255–281 952
920 34. Jean YC (1995) In: Dupasquier A, Mills AP Jr (eds) Positron 953
921 spectroscopy of solids. IOS Press, Amsterdam, pp 563–580 954
922 35. Tao S (1972) Positronium annihilation in molecular substances. J 955
923 Chem Phys 56:5499–5510 956
924
36. Eldrup M, Lightbody D, Sherwood J (1981) The temperature 925
dependence of positron lifetimes in solid Pivalic acid. Chem Phys 926
63:51–58 927
37. Consolati G (2002) Positronium trapping in small voids: influ- 928
ence of their shape on positron annihilation results. J Chem Phys 929
117:7279–7283 930
38. Hart E, Thomas J, Gordon S (1964) A review of the radiation 931
chemistry of single-carbon compounds and some reactions of the 932
hydrated electron in aqueous solution. Radiat Res Suppl 4:74–88 933
39. Stevens GC, Clarke RM, Hart EJ (1972) Radiolysis of aqueous 934
methane solutions. J Phys Chem 76:3863–3867 935
40. Hickel B (1975) Absorption spectra and kinetics of methyl and 936
ethyl radicals in water. J Phys Chem 79:1054–1059 937
41. Getoff N (1991) Radiation- and photoinduced degradation of 938
pollutants in water. A comparative study. Radiat Phys Chem 939
37:673–680 940
42. Ulanski P, Bothe E, von Sonntag C (1999) OH radical induced 941
depolymerization of poly(methacrylic acid). Nucl Instrum Meth- 942
ods Phys Res B 151:350–355 943
43. Ulanski P, Bothe E, Hildenbrand K, Rosiak JM, von Sonntag C 944
(1996) Hydroxyl-radical-induced reactions of poly(acrylic acid); 945
a pulse radiolysis, EPR and product study. Part I. Deoxygenated 946
aqueous solutions. J Chem Soc Perkin Trans 2:13 947
44. Janik I, Ulanski P, Rosiak JM, von Sonntag C (2000) Hydroxyl- 948
radical-induced reactions of the poly(vinyl methyl ether) model 949
2,4-dimethoxypentane in the absence and presence of dioxygen: 950
a pulse radiolysis and product study. J Chem Soc Perkin Trans 951
2:2034–2040 952
953
954
955
956